To be cited as: J. Phys. Chem. C, 2008, 112 (39), 15394–15401
DOI: 10.1021/jp803314c

Water in acid boralites: hydration effects on framework B sites.

Federica Trudu, Gloria Tabacchi, Aldo Gamba and Ettore Fois*

July 21, 2008

Dip. Scienze Chimiche ed Ambientali, University of Insubria at Como,

and INSTM udr Como, Via Lucini 3, I-22100 Como (Italy)

Abstract

Properties and behaviour of protonated boron-containing zeolites at different hydration degree have been investigated by means of periodic DFT approaches. Geometry optimization and room-temperature Car-Parrinello molecular dynamics results, in line with experimental findings, indicate that the BO_3-bound silanolic acid site typical of dry boralites should convert to a solvated H_3O^+ hydrogen bonded to tetrahedral BO_4 at moderate water content. By increase of the water loading, the tetrahedral structure of the B site is stabilized and the physicochemical properties of the water molecules solvating the acid proton gradually approach the liquid-phase ones. A relevant role of structural and vibrational properties of the zeolite framework in the water-induced trigonal-to-tetrahedral transition at the B site is highlighted by simulation results.

1 Introduction

Protonated boron containing zeolites[1] (*boralites*) have been the subject of growing interest due to their moderate acid strength. This feature is exploited in industrial processes, such as the Beckmann rearrangement[2,3] and the xylene isomerization,[4] requiring mild and shape-selective solid acid catalysts. Besides catalytic applications, these materials are appealing for fundamental research because, in contrast with standard framework cations, zeolitic boron may be found three- or four- coordinated depending on the degree of hydration. More specifically, in acid B-zeolites the coordination geometry at the

boron center changes from tetrahedral to trigonal upon dehydration. The tetrahedral structure is reversibly recovered upon rehydration, according to equation 1:[1]

$$\mathrm{Si-(OH)\cdots B(trigonal) + nH_2O \rightleftharpoons Si-O-B(tetrahedral) + (H_3O^+)_{aq}} \qquad (1)$$

Only proton-exchanged boralites are sensitive to this transition, while in the presence of other extraframework cations such as Na^+ framework boron is characterized by a stable tetrahedral geometry.[5] As indicated by a broad series of ^{11}B solid state NMR[5–10] and IR experiments,[11–19] B is characterized by a trigonal geometry in acid dry samples and a tetrahedral structure when contacted with water vapour, however, both tetra- and three- coordinated B sites can be co-present.[7,10,20] By washing with water, trigonal B can be hydrolyzed to a defective site up to full extraction from the framework (deboronation process).[1,5,9,10,15] The trigonal-to-tetrahedral B-site geometry change has also been detected by contacting acid boralites with other Brønsted bases, like pyridine, ammonia, ethanol, methanol.[20–22] On the other hand, non-polar molecules do not modify B coordination upon adsorption.[22] In spite of the wealth of studies on these systems, several details of the hydration-induced B coordination change still remain to be established. For instance, the correlation between water loading and structural modifications, or the reason why a tetrahedral B site is favored in presence of water have not been clarified yet.

The relationships between B site structure and its physico-chemical properties in anhydrous boralites have been recently investigated in a periodic DFT study, evidencing that the acid site could be described as a silanol group Si-OH weakly interacting with a planar BO_3 unit.[23] Such a silanol-like and loosely-bound character of the acid site, which is responsible of the lower acidity of boron zeolites with respect to their Al- and Ga counterparts,[24–26] implies long range framework perturbations, which may be related to the water-induced structural transition at the B site.

The protonation state determination of a zeolitic Brønsted acid site from first principles is not straightforward, even in the case of Al-(OH)-Si bridging groups in standard

aluminosilicates. Actually, no consensus has been reached yet about the number of water molecules needed to stabilize a hydronium ion inside a zeolitic cage.

In the past, calculations have been carried out by using a variety of first-principles techniques (both wavefunction- or electronic density-based) mainly on cluster models of zeolite acid sites.[27–31] First principles studies accounting for the periodicity of the crystal structure are available as well.[32–35]

Theoretical results agree in predicting that proton transfer from an Al-zeolite Brønsted acid site to a single water molecule does not occur; indeed, solvation of the hydronium ion by at least one water molecule is needed.[28,29,32] In the case of boron sites, whose acidity is lower, stabilization of hydronium species should require a larger number of solvating water molecules. Actually, a recent DFT study on a B-zeolite cluster model[30] evidenced that two water molecules are not effective in deprotonating the silanol group. Therefore, the conditions at which the structure with tetracoordinated B plus hydrated hydronium becomes energetically favored over the one with trigonal B plus hydrated silanol have not been established yet.

In the present work, model acid boralites characterized by different water content are studied by first principles periodic density functional (DFT) calculations, with the aim of gaining detailed insight into the water-induced B site trigonal-to-tetrahedral transition.

2 Computational Methods and Models

Sodalite is characterized by a unit cell stoichiometry [$Si_{12}O_{24}$] in the all silica form.[36] The unit cell is composed by two cubo-octahedral β cages,[37] which are the building blocks of several zeolites of widespread industrial use. Synthesis of B-sodalite samples (B-SOD) has been reported.[1] The cell parameters and unit-cell stoichiometry adopted in this work for the B-SOD framework are the same as in Ref.[23] to which the reader is referred for further details. Hydration effects on the B-site geometry were simulated

by progressively adding water molecules in a B-SOD model crystal containing one acid site, $H[BSi_{11}O_{24}]$. In particular, the simulated water loadings were as follows: i) one water molecule per unit cell, $H[BSi_{11}O_{24}] \cdot H_2O$ (B-SOD-1W), ii) two H_2O per cell, $H[BSi_{11}O_{24}] \cdot 2H_2O$ (B-SOD-2W); iii) four H_2O per cell, $H[BSi_{11}O_{24}] \cdot 4H_2O$; iv) five H_2O per cell, $H[BSi_{11}O_{24}] \cdot 5H_2O$ (B-SOD-5W); v) eleven H_2O per cell, $H[BSi_{11}O_{24}] \cdot 11H_2O$ (B-SOD-11W). With 4 H_2O per cell, two models were built: B-SOD-4W, where the 4 water molecules were placed in one β cage (cage a from now on), and B-SOD(3+1)W, with three H_2Os in cage a and one molecule in the adjacent cage (cage b from now on). System B-SOD-5W was modeled by positioning 5 water molecules in cage a, while system B-SOD-11W contains 6 molecules in cage a and 5 in cage b.

Geometry optimizations (GO) and first principles molecular dynamics (FPMD) simulations were carried out on the above described systems with the CPMD code.[38] Kohn-Sham orbitals were expanded in plane waves (PW) (Γ point only) and norm conserving[39] semilocal[40] Martins-Troullier pseudopotentials (with l=2 nonlocality) were employed for the ionic cores-valence electrons interactions.[41] GOs on the hydrated models were performed by quasi-Newton methods using mainly the Perdew-Burke-Ernzerhof (PBE)[42] gradient corrected density functional approximations, even though tests with other functionals (i.e. Becke[43]-Perdew[44] and HCTH/120[45]) were done as well. The PBE functional has been chosen because, besides its reliability in describing condensed phase systems, PBE energies and geometrical parameters for hydrogen bonded gas-phase complexes (e.g., small water clusters) compare rather well with results obtained with higher levels of theory.[46,47] Convergence of the results with respect to the kinetic energy cutoff in the PW expansion was checked by using cutoffs ranging from 70 to 110 Ry. Energy differences among minimum structures obtained from GOs at 70 Ry were calculated by taking into account the vibrational zero-point energy (zpe) contribution. Gibbs free energy differences ΔG at T=298.15 K were calculated as well, together with the corresponding spectroscopic entropy contribution $T\Delta S$, by using standard statis-

tical mechanics formulas.[48] As the investigated systems are solids, only the vibrational and electronic contributions to the partition function needed to be considered.[48] For B-SOD-4W system, zpe-corrected energy differences and thermodynamic quantities were calculated also at 90 and 110 Ry.

Car Parrinello[49] (CP) FPMD simulations were performed at room temperature conditions (NVT ensemble, Nose-Hoover chain thermostats with target ionic temperature of 300 K), with the PBE functional and a 70 Ry cutoff (PBE/70). Equilibration runs of 5 ps were performed by alternating 0.1 ps bins in the NVE ensemble by 0.1 ps bins with velocity rescaling. The Car Parrinello equations of motion[38,49] were integrated with a time step of 0.121 fs (5 a.u.). An inertia parameter of 500 a.u. was used for the electronic coefficients.

Finite temperature quantities were averaged over elapsed times of 15 ps. The dipole moments of the individual water molecules in the optimized structures were calculated by transforming the Kohn-Sham orbitals into maximally localized Wannier orbitals and assigning the centroids of the Wannier charge distributions (Wannier centers) to each water molecule.[50]

3 Results and discussion

3.1 Optimized structures

As discussed in the Introduction, in the presence of water, framework boron can be found either in a trigonal geometry loosely bound to a silanol (B^{III} from now on), or in a tetrahedral arrangement interacting with a solvated proton (B^{IV}). For each hydrated B-SOD model, full structural relaxations at different energy cutoff were performed on both B^{III} and B^{IV}-type structures. Relevant optimized geometrical parameters and energy differences are reported in Tables 1,2 and 3, where O* and Si* belong to the silanol group and O_w to the water molecule hydrogen-bonded to the silanol (see also ref.[23] for atom labels). These data indicate that optimizations provide converged struc-

tural results already at 70 Ry cutoff; moreover, changes in Kohn-Sham (KS) energy differences are within 0.5 kcal/mol in passing from 70 to 110 Ry, in line with the findings of Ref.[23] As reported in Table 3, inclusion of the zpe corrections does not alter the KS stability order, with the exception of the B-SOD-4W case. Interestingly, entropy effects, calculated at T=298.15, do not appear to be effective in changing the relative stability of the calculated minimum structures (Table 3).

No energy minimum has been found for the B^{IV}-type arrangements in the monohydrated and di-hydrated systems. In both optimized structures (Figures 1a-b), B is three coordinated and the silanol group is hydrogen bonded to one water molecule which acts as a proton acceptor. The water molecule ligated to the silanol is not hydrogen bonded to other framework oxygens.

In B-SOD-2W, the B^{III} structure with the silanol group is solvated by a water dimer (Figure 1b). One molecule is ligated to the silanol as in the B-SOD-1W system, and is hydrogen bonded to the second water which acts as a proton acceptor. The presence of a second water molecule induces a strenghtening of the hydrogen bond involving the silanol proton (see Table 1).

In B-SOD-(3+1)W, a linear chain of three water molecules is hydrogen-bonded to the silanol, while a fourth water is positioned at the center of the adjacent β cage (see Figure 1c). In contrast to the dimer in B-SOD-2W, here the water chain is connected to the framework oxygens via weak hydrogen bonds involving the terminal water molecule and is characterized by stronger inter-water interactions. So far, increase of the water content induces a shortening of the water-silanol hydrogen bond along with a lenghtening of the O*-H distance, while the geometry of the trigonal BO_3 unit remains essentially unaltered.

It is worth noticing that here, at difference with the mono- and di-hydrated systems, a relative minimum with the B^{IV}-type structure has been found (Figure 2a): a hydronium ion is strongly hydrogen-bonded to two water oxygens and, more weakly, to a

framework oxygen in the BO_4 unit (precisely to O*). The H_2Os interacting with H_3O^+ are not hydrogen bonded to the framework, like the fourth water molecule which is located at the neighboring β cage center. The BO_4 unit is characterized by a distorted tetrahedral geometry, with the B-O* bond significantly longer than the other three B-O bonds. Such a structure (Figure 2a) is slightly less stable than the silanolic form (Figure 1c) (1.87 kcal/mol at 70 Ry), and the energy difference decreases to 1.38 kcal/mol by inclusion of the zpe contribution.

Also when four water molecules are hosted in the same β cage in B-SOD-4W, both B^{III} and B^{IV}-type structures are found, however they are characterized by lower energies than the B-SOD-(3+1)W systems. In the B^{III}-type structure (see Figure 1d), the four water molecules form a closed chain (namely, a four-membered water ring (4WR)) connected to the silanol group via a strong hydrogen bond (1.602 Å). The other molecules in the chain do not interact with framework oxygens. Each water accepts a hydrogen bond from the neighboring molecule in the ring.

With tetracoordinated boron, two minima were found, separated by an energy difference of 4.33 kcal/mol. In the higher-energy arrangement, the hydronium is located relatively far from B (5.4 Å) and is solvated by three water molecules hydrogen bonded to framework oxygens. In the absolute B^{IV}-type minimum (Figure 2b), the hydronium is closer to B (3.5 Å) and hydrogen bonded to one oxygen of the BO_4 unit and two water molecules. Another water molecule is connected as a double acceptor to the H_2Os solvating the hydronium, thus forming a tight protonated 4WR structure. Remarkably, whereas without zero-point corrections this structure and the B^{III}-type one (Figure 1d) are nearly iso-energetic, inclusion of zpe stabilizes the form with hydrated hydronium plus tetrahedral boron. In particular, the zpe-corrected energy difference amounts to 1.91 kcal/mol at 70 Ry and the stability order is maintained also at higher cutoff. Interestingly, by inspecting the calculated harmonic frequencies it emerges that the higher zpe of the B^{III} structure is due to modes typical of trigonal B in a zeolite frame-

work. Indeed, the symmetric and asymmetric B-O-Si stretching modes are located in the regions around 900 and 1300 cm^{-1}, i.e. at significantly higher wavenumbers than those typical of a tetrahedral BO_4 unit (800 and 1180 cm^{-1}).

In B-SOD-5W, the absolute minimum structure is of the B^{IV}-type (Figure 2c). It is 3.38 kcal/mol lower in energy than the one with hydrated silanol and three-coordinated boron (Figure 1e). The energy difference rises to 4.48 kcal/mol upon inclusion of zpe contributions. In the B^{III}-type optimized structure, the silanol is hydrogen bonded to a neutral 4WR-cycle of water molecules. Six strong hydrogen bonds connect the water molecules among themselves and to the silanol group, while two weaker contacts are established between water protons and framework oxygens. The geometry of the boron site is very similar to the B-SOD-4W silanolic structure.

In the most stable B-SOD-5W structure, where boron is in a tetrahedral geometry, a protonated 4WR-cycle plus an hydrogen bonded water molecule (i.e., (4WR+1)-cluster) is detected (see Figure 2c). Besides five strong hydrogen bonds in the (4WR+1) cluster, five weaker ones connect the water ring to the framework. Both the hydronium and one of its first H_2O neighbors are hydrogen bonded to two oxygen atoms of the BO_4 unit. However, both the longer $H_3O^+ \cdots O^*$ hydrogen bond distances and the less distorted geometry of the BO_4 tetrahedron evidence that the interaction between hydronium and the boron site is weaker than in B-SOD-4W (see Table 2).

In the pentahydrated BO_4-plus-hydronium system we also found a minimum characterized by a protonated 5WR-cluster of one hydronium and four water molecules, which was 3.86 kcal/mol higher in energy than the B^{IV}-(4WR+1)-structure (3.06 kcal/mol with zpe). The microscopic origin of its lower stability should be the weaker hydrogen bonding network: indeed, here the 5WR-cluster is connected to the framework only by 3 weak hydrogen bonds.

At higher water loading, i.e. with 11 water molecules per boron site, the energy difference between the B^{IV} and B^{III}-type structures rises to -11.4 kcal/mol. Moreover, in line

with the tetra- and penta-hydrated systems, inclusion of the zpe corrections enhances the relative stability of the B^{IV}-type structure. In the structure with tetrahedral boron (Figure 2d), a protonated 5WR cluster, which contains the hydronium, is hydrogen bonded to a water molecule and a BO_4 oxygen. Moreover, a water molecule belonging to the 5WR is connected to another 5WR cluster located in the adjacent β-cage.
The B^{III}-type geometry (see Figure 1f) is characterized by a very large B-O* separation (2.836 Å), indicating that when a trigonal BO_3 unit is present, high water loadings cause significant distortions of the framework structure. Such a distortion may be one of the factors responsible of the lower stability of the B^{III}-type geometry at a high degree of hydration. Here the silanol oxygen is hydrogen bonded to a 4WR+1 cycle, with O* separated by 1.855 Å from a water proton, while the silanol proton interacts with a 5WR ring of water molecules located in the other β cage.

3.2 Dipole moment calculations

Analysis of the dipole moment of water molecules confined in zeolitic cavities could provide useful insight on the microscopic physico-chemical properties of hydrated zeolites. To the best of our knowledge, calculations of the dipole moment of water molecules interacting with a zeolitic Brønsted acid site are not available in the literature. However, the polarization of water molecules confined into a zeolite framework has been investigated by using classical MD[51,52] and recently also FPMD techniques.[53] In these studies, the water dipole was found to increase with hydration. In particular, in hydrophobic all-silica LTA containing 15 and 20 water molecules per unit cell the water dipole distributions obtained from FPMD were centered at 2.7 and 2.9 D respectively,[53] i.e. at values slightly smaller than bulk water (3.1 D) but significantly higher than in the gas phase (1.8 D). Such a result was attributed to water-water hydrogen bonding, which caused a larger self polarization of the confined water 'droplet' with increasing water content, while the framework contribution to H_2O polarization was found to play

a minor role.

The systems investigated in this work have lower hydration degree and an acid proton, however the calculated average dipole moments, which refer only to the neutral H_2O units, range from 2.5 to 3.3 D (see Table 4) and are generally in line with Ref.[53] The lowest value of the average dipole moment is obtained for the mono-hydrated system, and the average dipole generally tends to increase with the number of inter-water hydrogen bonds. In all cases the maximum value of the molecular dipole moment was calculated for the water molecule characterized by the strongest interaction with the silanol or the hydronium ion. Actually, due to the presence of an excess proton, at intermediate hydration degree (i.e., 4-5 water molecules) the average dipole moment may become even higher than that of confined water.[53] However, by further increasing the water loading to 11 molecules also the β cage *b*, which does not contain the acid proton, is filled and the average dipole moment decreases. Interestingly, the average dipole of the B^{IV}-type structure is always higher than that of the B^{III}-type geometry at the same water content. This suggests that acid protons in zeolites have an higher polarizing effect when they are in the solvated hydronium form. In the optimized B-SOD-(3+1)W geometries, the dipole moment of the single water molecule hosted in β cage *b* amounts to 1.90 and 2.05 D for the B^{III} and B^{IV} structures respectively. In both cases the dipole is closer to the gas phase value and significantly lower than that of the water molecule hydrogen bonded to the silanol (2.47 D). The higher dipole moment in the B^{IV}-type structure is due to the greater long-range polarizing effect of charge separation (namely, the hydronium ion and the BO_4 unit).

Further insight can be gained from the average dipole moment of the water molecules hosted in cage *a* calculated for the minimum energy structures at increasing water loading (Figure 3). At low hydration, the dipole steeply increases with the water content and presents a discontinuity at 4, where the B^{IV}-type structure, characterized by an higher average water dipole, becomes energetically favored over the B^{III} one. At higher

water loading the silanol-to-hydronium transition is fully accomplished, and the dipole increases asymptotically towards a value of 3.4 D. These results suggest therefore that, in order for the acid proton to leave the zeolite framework, the average dipole moment of the solvating water molecules should be higher than 3 D.

3.3 Room temperature simulations

FPMD simulations were performed on B-SOD model systems characterized by different level of hydration, using as starting configurations the corresponding minimum energy structures at 70 Ry cutoff. Due to the small energy difference between the B^{III}- and B^{IV}-type structures at intermediate hydration degree, two simulations (MD-4W-B^{III} and MD-4W-B^{IV}) were carried out in the case of B-SOD-4W, starting from the B^{III} and B^{IV} optimized geometries respectively.

The equilibrated structure resulting from each simulation closely resembled the corresponding energy minimum, with the mono and di-hydrated systems characterized by a silanol-like acid site, and the highly hydrated system B-SOD-11W by solvated hydronium and a tetrahedral B site. At intermediate water content, the average geometries obtained from the two B-SOD-4W simulations were close to the corresponding starting configurations, and no interconversion between the B^{III} and B^{IV}-type structures was observed along the trajectories, suggesting an interconversion activation barrier higher than KT.

Detailed information on the structure and behaviour of boron sites at room temperature conditions can be gathered by the analysis of the pair correlation functions (rdf) obtained from the FPMD simulations. The B-O rdf calculated for the B-SOD systems at low (MD-1W, MD-2W), medium (MD-4W-B^{III}, MD-4W-B^{IV}) and high (MD-11W) degree of hydration are represented in Figure 4, where also the B-O rdf corresponding to the dry model system[23] has been shown for comparison. When a B^{III}-type geometry is present, namely in MD-dry, MD-1W, MD-2W and MD-4W-B^{III}, the rdf shows a sharp peak at 1.37 Å and a broader second peak centered at 2.65, 2.68, 2.76 and 2.80

Å respectively. The two peaks, which integrate to three and one, correspond to the three B-O bond distances in the trigonal BO_3 unit and to the loose contact between B and the silanol oxygen O* respectively. The B-O* peak is always located at distances about 5-10% longer than in the corresponding minimum structures, suggesting that thermal effects on the structural arrangement of the weakly interacting groups Si*-O*H and BO_3 are also relevant at very low or moderate water content (Table 5). Also the standard deviation of the B-O* mean distance, larger than those of the other B-O bonds, indicates larger thermal fluctuations of this contact. Interestingly, such an effect becomes more pronounced by increasing the water content, as indicated by the progressive broadening and shift towards longer distances of the B-O* peak in the 1W-2W-4W sequence. This picture drastically changes in passing to the B^{IV}-type systems, namely MD-4W-B^{IV} and MD-11W. Here, at short distances the B-O rdf's show only one sharp peak, integrating to four and centered at 1.47 Å. Such a peak corresponds to the four B-O bonds of the tetrahedral BO_4 unit. The calculated B-O bond distance, averaged over the four tetrahedral bonds, amounted to 1.487 and 1.483 Å for MD-4W-B^{IV} and MD-11W respectively. Their fluctuations (0.06 and 0.05 Å) are larger than those of the B-O bonds in the B-^{III} structures. Indeed, during both MD-4W-B^{IV} and MD-11W simulations, the hydronium ion remained in contact with the BO_4 unit, however, the framework oxygen acting as hydrogen-bonding partner was observed to change along the trajectory. Structural differences between moderate and high water loading are only detectable in the second neighbour shell: with four water molecules, the rdf shows two peaks at 3.42 and 3.79 Å, while in system B-SOD-11W only a peak at 3.79 Å is present.

Further information on the behaviour of the model system with increasing water loading can be drawn by analyzing water-framework and water-water rdf's and coordination numbers. As reported in Table 6, the average number of hydrogen bonds per water molecule increases with the water loading, as well as the water-framework oxygens

contacts. However, water-water hydrogen bonds are in general stronger than the water-framework oxygens ones: while all O_w-O_w rdf's of the poly-hydrated systems show a sharp peak at distances below 2.75 Å, the O_w-O_f rdf are characterized by a broad and shallower peak in the hydrogen-bonding region (See Figure 5).

When a B^{III}-type structure is present, a strong and stable hydrogen bond always connects the silanol proton and a solvating water molecule. In contrast, interactions among water and framework oxygens become significant only when the water content is at least four water molecules per acid site. As expected on the basis of the geometry optimizations results, the water-water separation becomes shorter in passing from the MD-2W to the MD-4W-B^{III} systems, and also from MD-4W-B^{III} to MD-4W-B^{IV} (Figure XY). Therefore, also at room temperature conditions both the increase of water content in cage *a* and the transition from silanol acid site to caged solvated hydronium contribute to strenghten the inter-water hydrogen bonding network. At higher hydration degree, the water-water separation seems to slightly increase due to the filling of the β cage *b*, which does not contain the hydronium ion and is therefore characterized by longer inter-water hydrogen bonds. Moreover, the peak height decreases significantly in passing from MD-4W-B^{IV} to MD-11W and the values of the rdf maximum (4.2) and position (2.59 Å) become closer to those obtained for liquid water by using the same DFT approximation and PW cutoff[47] (2.99 and 2.70 Å respectively).

4 Conclusions

The effect of water on boron sites in acid boralites has been studied by means of periodic DFT approaches on model B-zeolites characterized by different hydration degree. Results of both geometry optimizations and first principles molecular dynamics simulations indicate that the tetrahedral B plus hydrated hydronium arrangement becomes favored over the B-trigonal plus silanol form when at least four water molecules are available to solvate the acid proton, and that its stabilization increases with the hy-

dration degree.

Vibrational zero point effects may be very important for the relative stability of the B^{III}- B^{IV}-type forms at the transition point, i.e. where a moderate water content is present and the two structures of the B site are very close in energy. In particular, the stabilization of the tetrahedral-B plus hydronium form is mainly due to the different contribution to the zero point energy of the vibrational modes of the BO_3 (900 and 1300 cm^{-1}) and BO_4 (800 and 1180 cm^{-1}) units. This finding suggests that the relevance of zpe contributions in determining the acid site structure at moderate hydration degree might be a feature typical of B zeolites.

During the room temperature FPMD simulations no conversion between the B^{III} and B^{IV}-type structures was observed, suggesting that the water-induced trigonal-to-tetrahedral transition at the B site should be an activated process.

Analysis of the dipole moment of the caged water molecules highlighted a significant polarizing effect of the acid proton on confined water molecules, which is higher for the solvated hydronium form. At moderate hydration degree, additional solvent molecules contribute to increase water polarization. At high water loading, calculated average dipole moments and O(water)-O(water) pair correlation functions show how the properties of the confined water system become closer to those of liquid water.

Model	B-O*	B-O1	B-O$^{\#}$	B-O2	O*-H	H-O$_w$	Si*-O*	B-Si*	B-O*-Si*
dry									
PBE/70	2.574	1.373	1.371	1.358	0.974	-	1.639	3.938	137.3
1W									
PBE/70	2.588	1.371	1.370	1.362	0.996	1.801	1.627	3.953	138.2
PBE/90	2.605	1.369	1.366	1.359	0.991	1.800	1.625	3.974	138.8
PBE/110	2.608	1.368	1.367	1.359	0.991	1.796	1.625	3.979	138.9
2W									
PBE/70	2.596	1.378	1.363	1.367	1.016	1.652	1.620	3.948	137.7
PBE/90	2.605	1.370	1.360	1.365	1.004	1.678	1.620	3.957	137.8
PBE/110	2.612	1.374	1.360	1.364	1.005	1.671	1.619	3.964	137.8
(3+1)W									
PBE/70	2.546	1.385	1.361	1.362	1.022	1.582	1.616	3.936	141.1
PBE/90	2.545	1.383	1.357	1.359	1.015	1.590	1.614	3.938	141.4
PBE/110	2.530	1.384	1.357	1.358	1.015	1.587	1.614	3.919	141.0
4W									
PBE/70	2.534	1.378	1.376	1.344	1.022	1.593	1.613	3.963	144.8
PBE/90	2.542	1.375	1.374	1.341	1.015	1.601	1.612	3.968	144.7
PBE/110	2.543	1.375	1.375	1.342	1.015	1.602	1.612	3.970	144.7
5W									
PBE/70	2.532	1.377	1.375	1.355	1.018	1.594	1.614	3.956	144.3
PBE/90	2.531	1.375	1.373	1.354	1.011	1.600	1.612	3.956	144.5
PBE/110	2.523	1.375	1.372	1.352	1.010	1.602	1.612	3.951	144.7
11W									
PBE/70	2.836	1.376	1.361	1.336	0.989	1.855	1.640	4.130	132.8
PBE/90	2.844	1.375	1.358	1.332	0.984	1.802	1.642	4.126	132.0
PBE/110	2.844	1.374	1.358	1.332	0.984	1.805	1.640	4.126	132.0

Table 1: Relevant geometrical parameters for the B^{III}-type optimized geometries (three-coordinated B site plus silanol) at different hydration degree. O_w indicates the oxygen atom of the water molecule hydrogen bonded to the silanol proton.

Model	B-O*	B-O1	B-O$^{\#}$	B-O2	O*$\cdots$H	H-O_{H+}	B-O_{H+}	Si*-O*	B-Si*	B-O*-Si*
(3+1)W										
PBE/70	1.529	1.455	1.482	1.456	1.687	1.021	3.311	1.618	3.037	149.5
PBE/90	1.529	1.454	1.479	1.459	1.701	1.014	3.315	1.617	3.037	149.7
PBE/110	1.526	1.453	1.478	1.458	1.703	1.014	3.315	1.616	3.036	150.0
4W										
PBE/70	1.534	1.456	1.491	1.457	1.592	1.024	3.573	1.628	2.944	137.1
PBE/90	1.530	1.453	1.490	1.456	1.606	1.020	3.572	1.626	2.941	137.4
PBE/110	1.526	1.452	1.489	1.456	1.609	1.020	3.572	1.626	2.938	137.5
4W'										
PBE/70	1.518	1.441	1.492	1.451	1.635	1.108	5.398	1.619	3.028	149.7
PBE/90	1.515	1.441	1.490	1.449	1.649	1.099	5.387	1.617	3.025	150.1
PBE/110	1.513	1.441	1.490	1.450	1.654	1.099	5.388	1.617	3.024	150.1
5W										
PBE/70	1.518	1.455	1.482	1.463	1.699	1.016	3.476	1.615	2.981	144.2
PBE/90	1.514	1.452	1.482	1.461	1.714	1.008	3.472	1.612	2.983	145.4
PBE/110	1.511	1.453	1.481	1.460	1.720	1.007	3.470	1.610	2.984	145.8
5W'										
PBE/70	1.523	1.454	1.494	1.460	1.793	1.001	3.195	1.620	2.970	141.8
PBE/90	1.516	1.454	1.495	1.456	1.807	0.996	3.198	1.618	2.965	142.2
PBE/110	1.515	1.453	1.493	1.457	1.810	0.994	3.200	1.618	2.966	142.3
11W										
PBE/70	1.506	1.452	1.502	1.475	1.716	1.003	3.245	1.622	3.019	150.1
PBE/90	1.504	1.451	1.501	1.471	1.741	0.997	3.254	1.621	2.968	143.5
PBE/110	1.502	1.451	1.500	1.471	1.742	0.996	3.252	1.620	2.967	143.7

Table 2: Relevant geometrical parameters for the B^{IV}-type optimized geometries (i.e. tetracoordinated B site plus hydronium) at different water content. 4W' and 5W' indicate higher-energy minima for B-SOD-4W and B-SOD-5W systems respectively. The label O_{H+} refers to the oxygen atom of the hydronium ion.

	$\Delta E^{\mathrm{IV-III}}$(KS)	$\Delta E^{\mathrm{IV-III}}$(KS+zpe)	$T\Delta S$	ΔG
B-SOD-(3+1)W				
PBE/70	1.87	1.38	-2.71	2.92
PBE/90	2.33			
PBE/110	2.42			
B-SOD-4W				
PBE/70	0.08	-1.91	-2.73	-1.53
PBE/90	-0.04	-2.41	0.13	-2.47
PBE/110	-0.15	-1.26	-1.74	-0.11
B-SOD-5W				
PBE/70	-3.38	-4.48	-1.15	-3.76
PBE/90	-3.54			
PBE/110	-3.48			
B-SOD-11W				
PBE/70	-11.85	-13.18	-2.88	-11.55
PBE/90	-11.47			
PBE/110	-11.41			

Table 3: Kohn-Sham and zpe corrected energy differences ΔE, entropy contributions to the Gibbs free energy differences $T\Delta S$ and Gibbs free energy differences ΔG calculated for the B^{IV} and B^{III}-type structures at different hydration degree. Values in kcal/mol. T=298.15 K.

	$< \mu >$	μ_{max}
B-SOD-1W(III)	2.47	2.47
B-SOD-2W(III)	2.85	2.93
B-SOD-(3+1)W(III)	2.69 (2.96)	3.29
B-SOD-(3+1)W(IV)	2.81 (3.20)	3.45
B-SOD-4W(III)	3.10	3.34
B-SOD-4W(IV)	3.27	3.37
B-SOD-5W(III)	3.05	3.27
B-SOD-5W(IV)	3.28	3.46
B-SOD-11W(III)	2.93 (2.95)	3.10
B-SOD-11W(IV)	3.17 (3.32)	3.74

Table 4: Average dipole moments of the water molecules solvating the acid proton $< \mu >$ and dipole moment of the water molecule closest to the acid proton μ_{max}. Values in parenthesis are averaged over the molecules hosted in cage *a*. Dipole moments (in D) are calculated for the structures optimized at 110 Ry cutoff.

	B-O*	B-O1	B-O#	B-O2
MD-dry	2.711 (0.19)	1.373 (0.03)	1.375 (0.03)	1.356 (0.03)
MD-1W	2.713 (0.16)	1.372 (0.03)	1.374 (0.03)	1.357 (0.03)
MD-2W	2.763 (0.17)	1.375 (0.03)	1.382 (0.03)	1.362 (0.03)
MD-4W$^{(III)}$	2.794 (0.21)	1.384 (0.03)	1.364 (0.03)	1.351 (0.03)
MD-4W$^{(IV)}$	1.465 (0.05)	1.496 (0.07)	1.503 (0.07)	1.482 (0.05)
MD-11W	1.484 (0.05)	1.479 (0.05)	1.479 (0.05)	1.489 (0.05)

Table 5: Selected mean geometrical parameters and relative standard deviations (in parenthesis) for the dry and hydrated B-SOD systems at the PBE/70 level. Distances in Å.

	n_w^a	n_f^a	n_w^d	n_f^d
MD-1W	1.00	0.00	0.00	1.00
MD-2W	1.00	0.00	0.50	1.00
MD-4W(III)	1.25	0.00	1.00	1.00
MD-4W(IV)	1.25	0.30	1.25	0.00
MD-11W	1.50	0.75	1.60	0.00

Table 6: Number of hydrogen bonds per molecule in which water participates as an acceptor (n_w^a) and as a donor (n_w^d); number of hydrogen bonds per framework oxygen in which the framework participates as an acceptor (n_f^a). The number of hydrogen bonds in which the framework participates as a donor (n_f^d) is one in the B^{III}-type structures and zero otherwise.

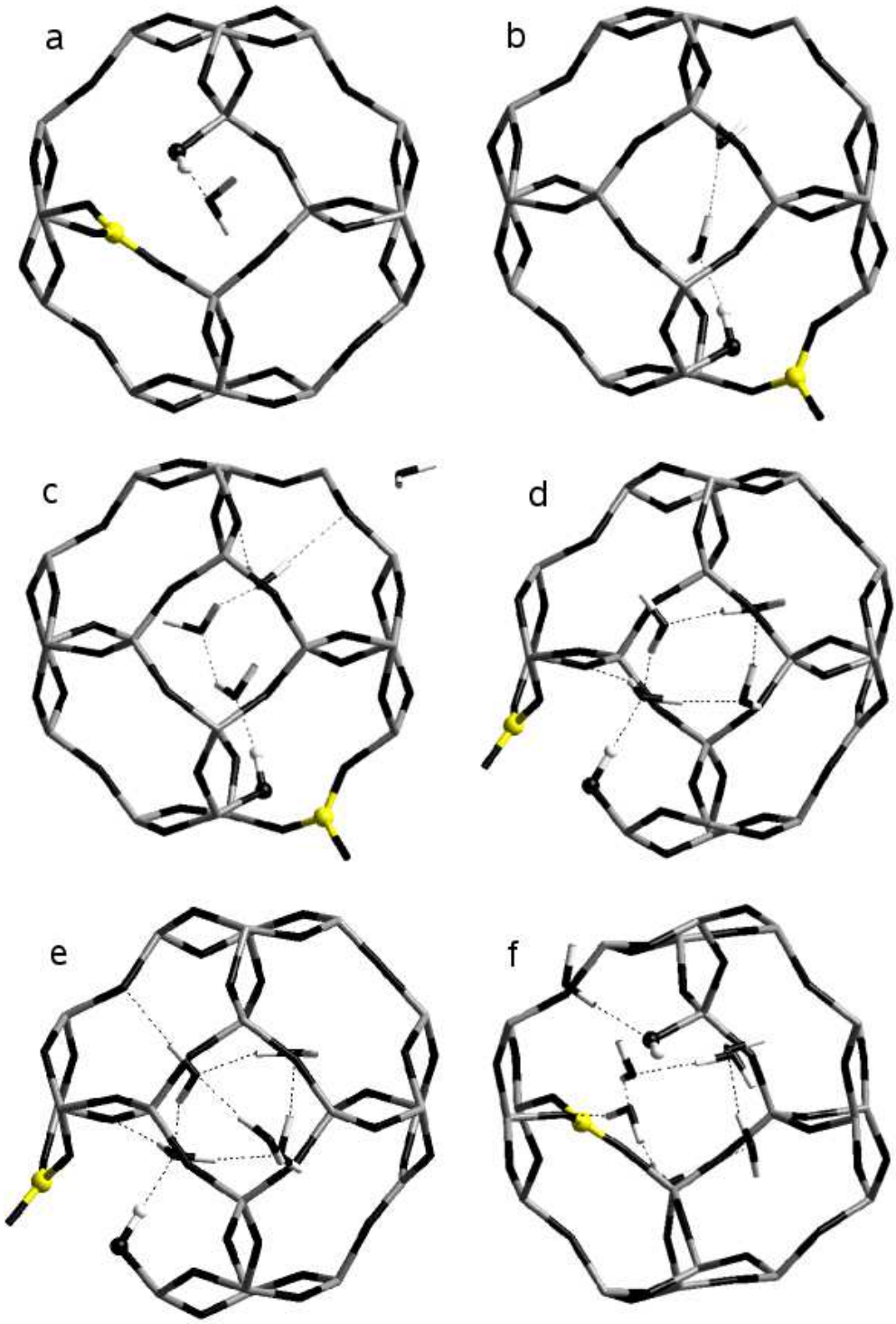

Figure 1: Graphical representation of the B^{III}-type optimized structures at different water content. a: B-SOD-1W; b: B-SOD-2W; c: B-SOD-(3+1)W; d: B-SOD-4W; e: B-SOD-5W; f: B-SOD-11W. For clarity, in the case of the B-SOD-11W structure only water molecules in cage *a* are represented. Atom labeling: Oxygen atoms: black sticks; silicon atoms: gray sticks; protons: light gray sticks. B atoms are represented as yellow spheres. The silanol group is represented with spheres.

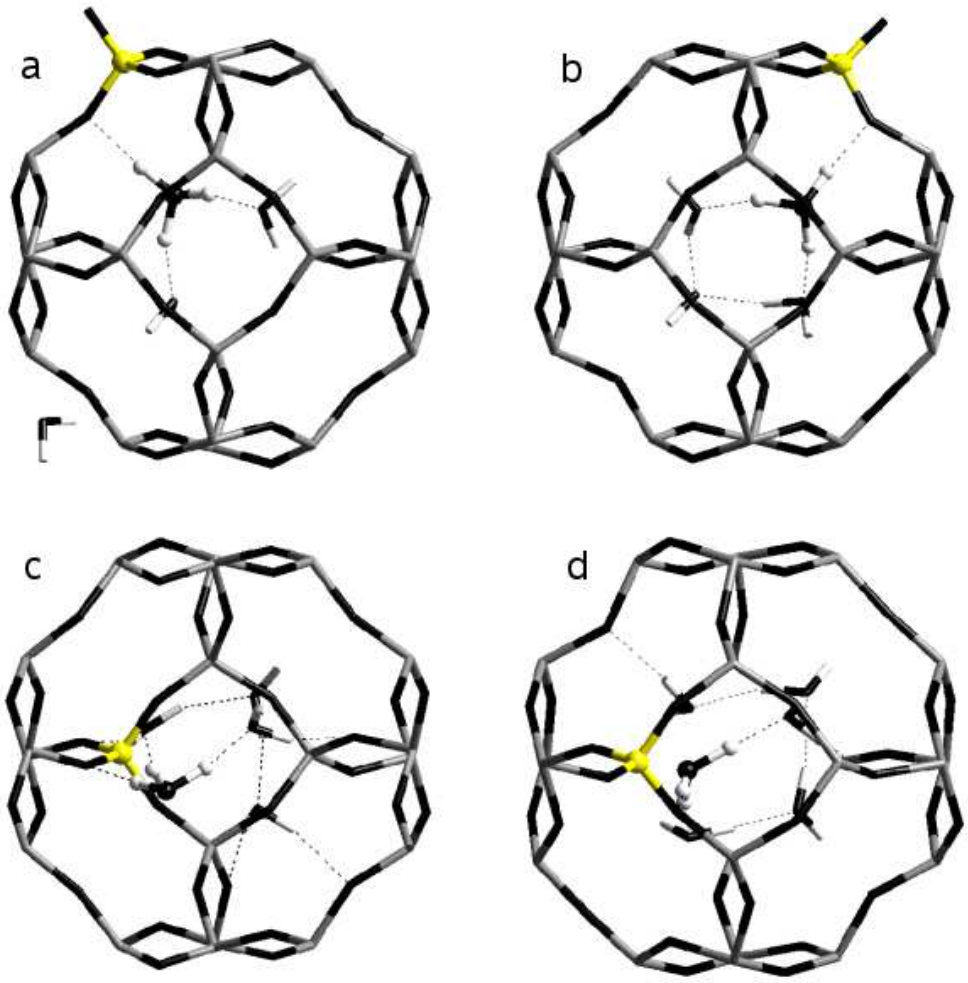

Figure 2: Graphical representation of the B^{IV}-type optimized structures at different water content. a: B-SOD-(3+1)W; b: B-SOD-4W; c: B-SOD-5W; d: B-SOD-11W. For clarity, in the case of the B-SOD-11W structure only water molecules in cage *a* are represented. Atom labeling: Oxygen atoms: black sticks; silicon atoms: gray sticks; protons: light gray sticks. B atoms are represented as yellow spheres. The hydronium ion is represented with spheres.

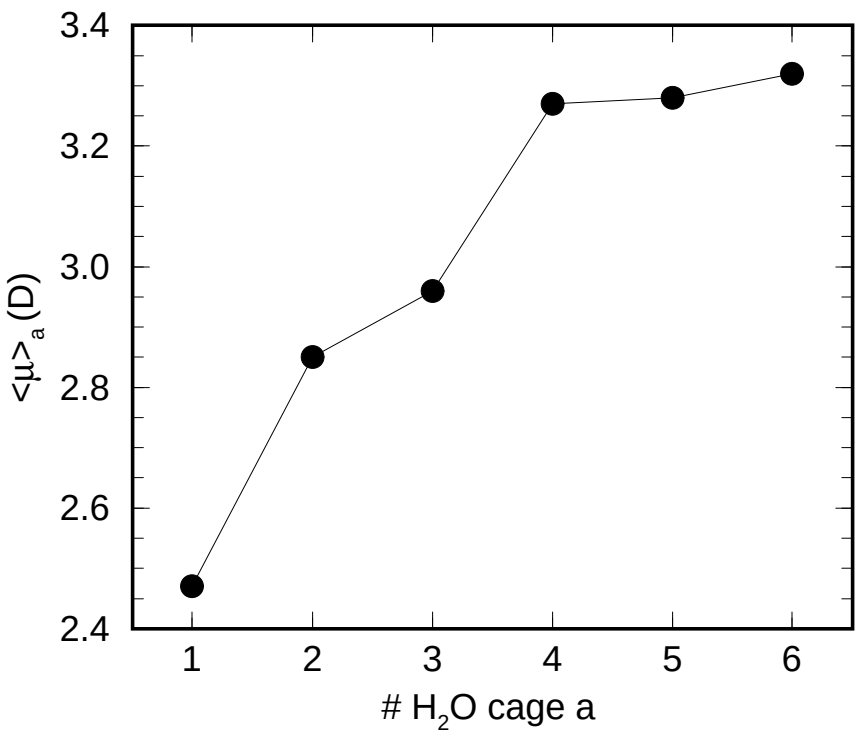

Figure 3: Calculated average dipole moments of water molecules in cage a as a function of the number (#) of water molecules in cage a.

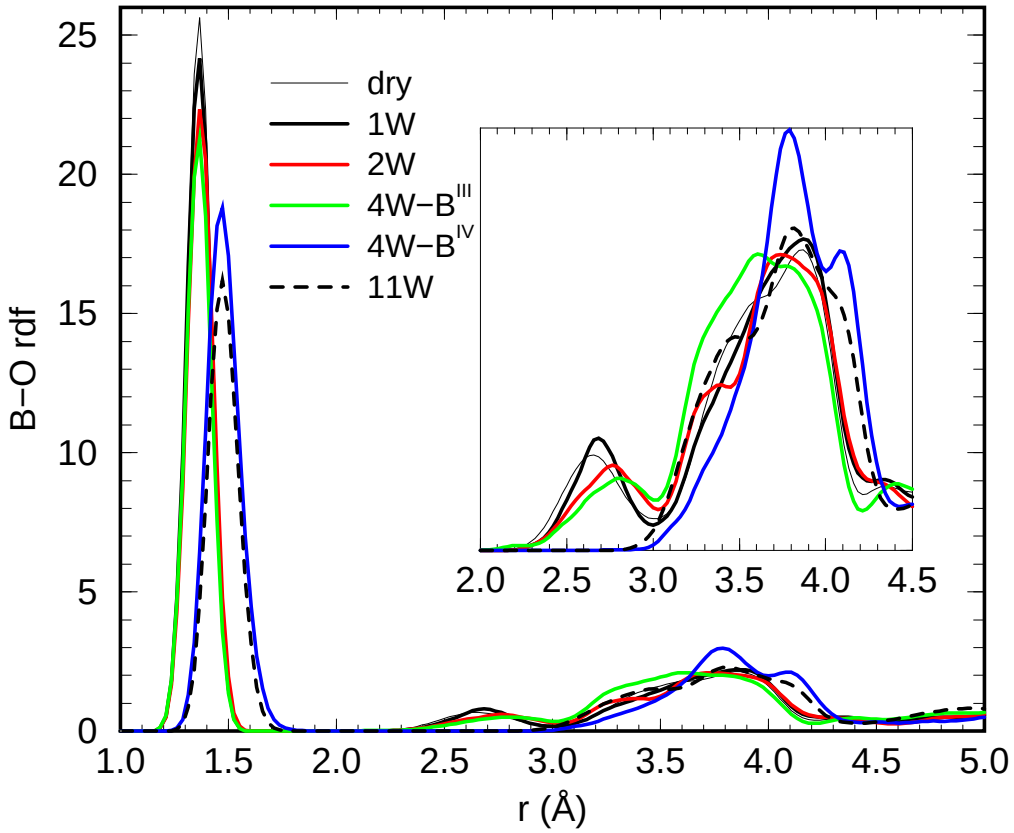

Figure 4: B-O radial distribution functions rdf for B-SOD systems at different hydration degree.

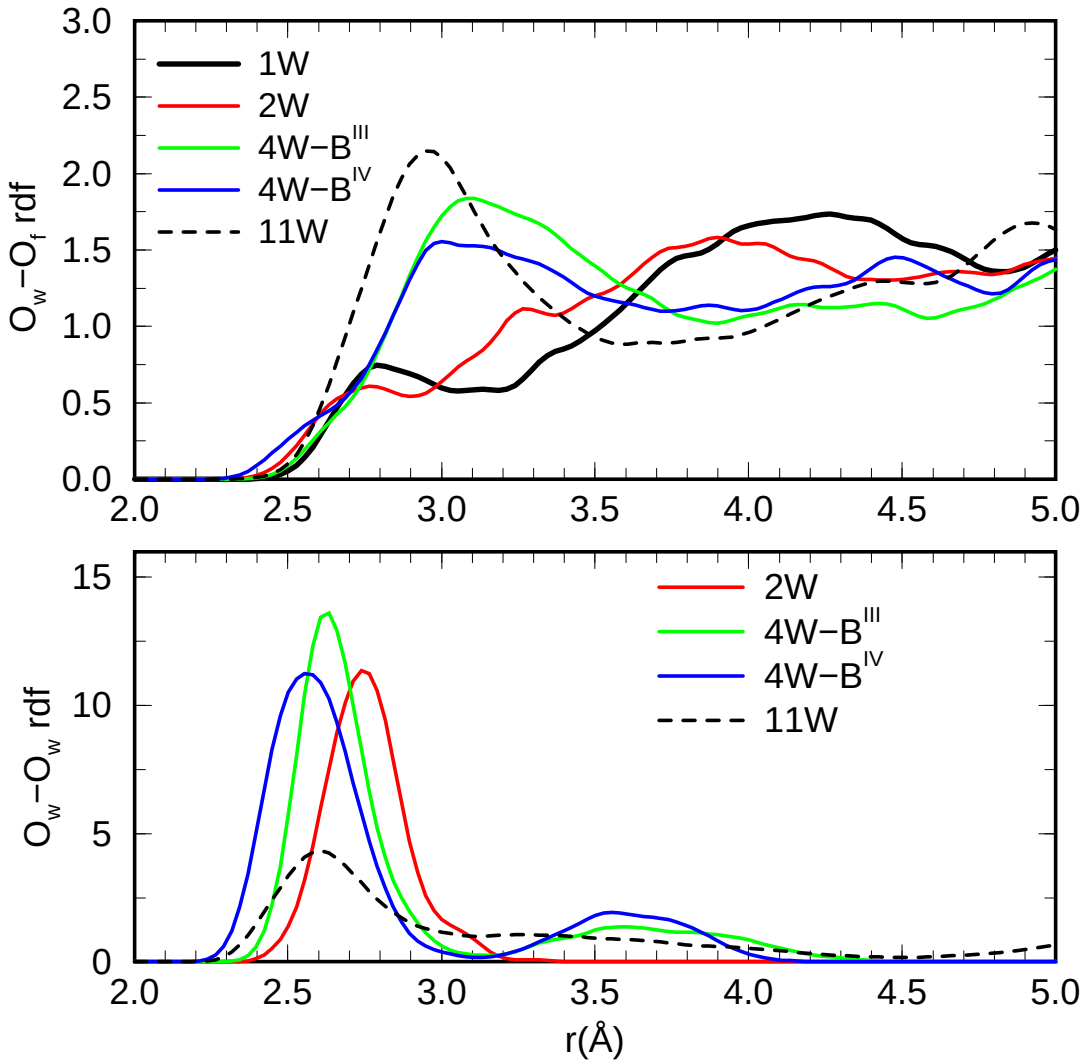

Figure 5: Water oxygen-framework oxygens (top panel) and water oxygen-water oxygen (bottom panel) radial distribution functions rdf.

References

1. Millini, R.; Perego, G.; Bellussi, G. *Top. Catal.* **1999,** *9,* 13-20.

2. Roeseler, J.; Heitmann, G.; Hölderich, W. . In *Progress in Zeolites and Microporous Materials, Studies in Surface Science and Catalysis*, Vol. 105; Chon, H.; Ihm, S.-K.; Uh, Y. S., Eds.; Elsevier: Amsterdam, 1997.

3. Forni, L.; Fornasari, G.; Trifiro', F.; Aloise, A.; Katovic, A.; Giordano, G.; Nagy, J. B. *Microp. Mesopor. Mater.* **2007,** *101,* 161-168.

4. Hölderich, W. . In *New Developments in Zeolite Science and Technology, Studies in Surface Science and Catalysis*, Vol. 28; Murakami, Y.; Ijima, A.; Ward, I. J., Eds.; Elsevier: Amsterdam, 1986.

5. Koranyi, T. I.; Nagy, J. B. *J. Phys. Chem. B* **2006,** *110,* 14728-14735.

6. Scholle, J.; Veeman, W. S. *Zeolites* **1985,** *5,* 118.

7. Fild, C.; Shantz, D. F.; Lobo, R. F.; Koller, H. *Phys. Chem. Chem. Phys.* **2000,** *2,* 3091-3098.

8. Chen, L.; Zhang, M.; Yue, Y.; Ye, C.; Deng, F. *Micropor. Mesopor. Mater.* **2004,** *76,* 151-156.

9. Hwang, S. J.; Chen, C. Y.; Zones, S. I. *J. Phys. Chem. B* **2004,** *108,* 18535-18546.

10. Koller, H.; Fild, C.; Lobo, R. F. *Micropor. Mesopor. Mater.* **2005,** *79,* 215-224.

11. Coudurier, G.; Vedrine, J. C. *Pure Appl. Chem.* **1986,** *58,* 1389-1396.

12. Kessler, H.; Chereau, J. M.; Guth, J. L.; Strub, H.; Coudurier, G. *Zeolites* **1987,** *7,* 360-366.

13. Datka, J.; Piwowarska, Z. *J Chem. Soc. Faraday Trans.* **1989,** *85,* 47-53.

14. Cichocki, A.; Datka, J.; Olech, A.; Piwowarska, Z.; Michalik, M. *J Chem. Soc. Faraday Trans.* **1990,** *86,* 753-756.

15. Cichocki, A.; Lasocha, W.; Michalik, M.; Sawlowicz, Z.; Bui, M. *Zeolites* **1990,** *10,* 583-587.

16. Testa, F.; Chiappetta, R.; Crea, F.; Aiello, R.; Fonseca, A.; Nagy, J. B. *Studies Surf. Sci. Catal.* **1995,** *94,* 349-355.

17. Zhou, W.; Zhang, S. Y.; Hao, X. Y.; Guo, H.; Zhang, C.; Zhang, Y. Q.; Liu, S. *J. Sol. State Chem.* **2006,** *58,* 855-865.

18. Scarano, D.; Zecchina, A.; Bordiga, S.; Geobaldo, F.; Spoto, G.; Petrini, G.; Leofanti, G.; Padovan, M.; Tozzola, G. *J. Chem. Soc. Faraday Trans.* **1993,** *89,* 4123-4130.

19. Regli, L.; Bordiga, S.; Lamberti, C.; Lillerud, K. P.; Zones, S. I.; Zecchina, A. *J. Phys. Chem. C* **2007,** *111,* 2992-2999.

20. Mihály, R. M.; Pál-Borbely, G.; Beyer, H. K.; Szegedi, A.; Koráyi, T. I. *Micropor. Mesopor. Mater.* **2007,** *98,* 132-142.

21. Marthala, V. R.; Wang, W.; Jiao, J.; Jiang, Y.; Huang, J.; Hunger, M. *Micropor. Mesopor. Mater.* **2007,** *99,* 91-97.

22. Axon, S. A.; Klinowski, J. *J. Phys. Chem.* **1994,** *98,* 1929.

23. Trudu, F.; Tabacchi, G.; Gamba, A.; Fois, E. *J. Phys. Chem. A* **2007,** *111,* 11626-11637.

24. Chu, C. T. W.; Chang, C. D. *J. Phys. Chem.* **1985,** *89,* 1569-1571.

25. Fois, E.; Gamba, A.; Tabacchi, G. *J. Phys. Chem. B* **1998,** *102,* 3974-3979.

26. Fois, E.; Gamba, A.; Tabacchi, G. *Phys. Chem. Chem. Phys.* **1999,** *1,* 531-536.

27. Krossner, M.; Sauer, J. *J. Phys. Chem.* **1996,** *100,* 6199.

28. Zygmunt, S. A.; Curtiss, L. A.; Iton, L. E. *J. Phys. Chem. B* **2001,** *105,* 3034-3038.

29. Limtrakul, J.; Chuichay, P.; Nokbin, S. *J. Mol. Struct.* **2001,** *560,* 169-177.

30. Goursot, A.; Berthomieu, D. *Magn. Reson. Chem.* **2004,** *42,* S180-S186.

31. Wang, Y.; Zhou, D.; Yang, G.; Miao, S.; Liu, X.; Bao, X. *J. Phys. Chem. A* **2004,** *108,* 6730-6734.

32. Nusterer, E.; Blöchl, P. E.; Schwarz, K. *Chem. Phys. Lett.* **1996,** *253,* 448-455.

33. Termath, V.; Haase, F.; Sauer, J.; Hutter, J.; Parrinello, M. *J. Am. Chem. Soc.* **1998,** *120,* 8512-8516.

34. Benco, L.; Demuth, T.; Hafner, J.; Hutschka, F. *Chem. Phys. Lett.* **2000,** *324,* 373-380.

35. Demuth, T.; Benco, L.; Hafner, J.; Toulhoat, H. *Int. J. Quantum Chem.* **2001,** *84,* 110-116.

36. Bibby, D. M.; Dale, M. P. *Nature* **1985,** *317,* 157-163.

37. Baerlocher, C.; Meier, W. M.; Olson, D. H. *Atlas of Zeolite Framework Types;* Elsevier: The Netherlands, 2001.

38. www.cpmd.org, *CPMD code;* : MPI für Festkörperforschung, Stuttgart, and IBM Zürich Research Laboratory, 1990-2007.

39. Hamann, D. R.; Schlüter, M.; Chiang, C. *Phys. Rev. Lett.* **1979,** *43,* 1494-1497.

40. Kleinman, L.; Bylander, D. M. *Phys. Rev. Lett.* **1982,** *48,* 1425-1428.

41. Troullier, N.; Martins, J. L. *Phys. Rev. B* **1991,** *43,* 1993-2006.

42. Perdew, J. P.; Burke, K.; Ernzerhof, M. *Phys. Rev. Lett.* **1996,** *77,* 3865-3868.

43. Becke, A. D. *Phys. Rev. A* **1988,** *38,* 3098-3100.

44. Perdew, J. P. *Phys. Rev. B* **1986,** *33,* 8822-8824.

45. Hamprecht, F. A.; Cohen, A. J.; Tozer, D. J.; Handy, D. J. *J. Chem. Phys.* **1998,** *109,* 6264-6271.

46. Ireta, J.; Neugebauer, J.; Scheffler, M. *J. Phys. Chem. A* **2004,** *108,* 5692.

47. Todorova, T.; Seitsonen, A. P.; Hutter, J.; Kuo, I.-F. W.; Mundy, C. J. *J. Phys. Chem. B* **2006,** *110,* 3685.

48. McQuarrie, D. A. *Statistical Mechanics;* Univ. Science Books: Herndon, VA, USA, 2000.

49. Car, R.; Parrinello, M. *Phys. Rev. Lett.* **1985,** *55,* 2471-2474.

50. Silvestrelli, P. L.; Marzari, N.; Vanderbilt, D.; Parrinello, M. *Solid State Commun.* **1998,** *107,* 7.

51. Smirnov, K. S.; Bougeard, D. *Chem. Phys.* **2003,** *292,* 53-70.

52. Shirono, K.; Daiguji, H. *Chem. Phys. Lett.* **2006,** *417,* 251-255.

53. Coudert, F.-X.; Vuilleumier, R.; Boutin, A. *ChemPhysChem* **2006,** *7,* 2464-2467.